

Electronic Supplementary Information

Intra-Surface Plasmon Coupling between Smooth and Nanoporous Blocks in a Gold Nanorod

Hye-Mi Bok,^a Kevin L. Shuford,^{‡c} Eden Jeong^a and Sungho Park^{*ab}

^aDepartment of Chemistry & Department of Energy Science &

^bSKKU Advanced Institute of Nanotechnology, Sungkyunkwan University, Suwon,
440-746, South Korea.

Fax: 82-31-290-7075; Tel: 82-31-299-4562; E-mail: spark72@skku.edu

^cChemical Science Division, Oak Ridge National Laboratory, P.O. Box. 2008 MS6142,
Oak Ridge, TN 37831, USA

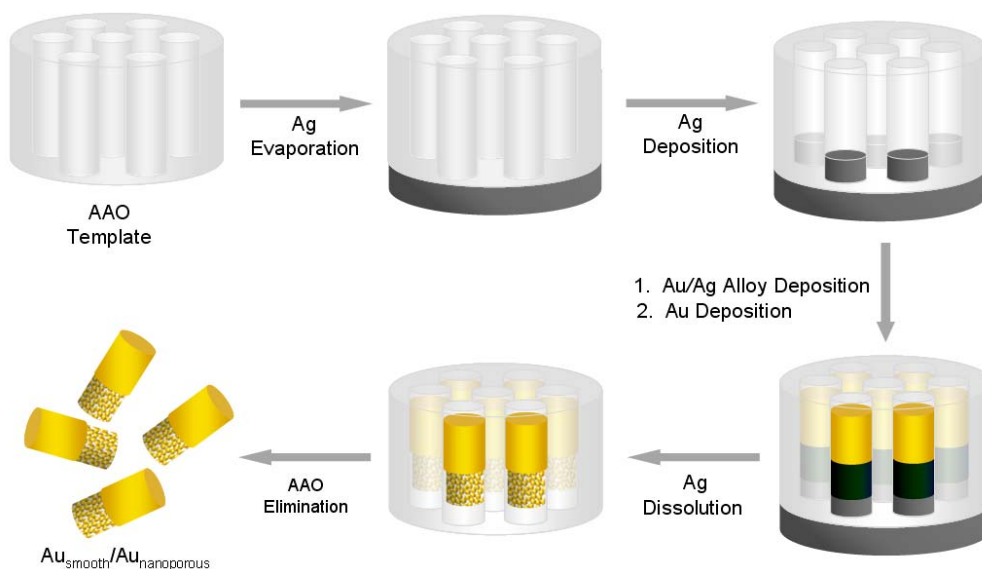
[‡]Current address: Department of Chemistry, Drexel University, 3141 Chestnut Street,
Philadelphia, PA 19104

Synthetic Approach

AAO Synthesis: The synthetic procedure is based on the method established by Masuda et al (ref. H. Masuda and K. Fukuda, *Science*, 1995, **268**, 1466.). An AAO template with 85 (± 5 nm) diameter pores was synthesized through a two-step anodization process. A piece of aluminum plate ($3.5 \times 5.0 \text{ cm}^2$) served as the anode while graphite served as the cathode in the two-electrode electrochemical cell. A high-purity (99.999%) thin sheet of aluminum (from Goodfellow Cambridge Limited) was electropolished with a mixture of ethanol and perchloric acid (7/3, v/v) at +20 V. Mirror-reflective shiny aluminum was anodized in 0.3 M oxalic acid (from Sigma-Aldrich) at 40 V and 0°C for 12 hours. The alumina layer was removed in a mixture of chromic acid (from Sigma-Aldrich) (1.8 wt%) and phosphoric acid (from Samchun Chemical) (6 wt %), at 60 °C for 12 hours. A second anodization step followed in 0.3 M oxalic acid at 40 V and 0 °C for 24 hours, producing highly ordered porous AAO template. The residue of aluminum plate was next removed by immersing in saturated HgCl₂ aqueous solution for 6 hours and then immersed in 8.5 wt % phosphoric acid solution for pore widening for 30 min.

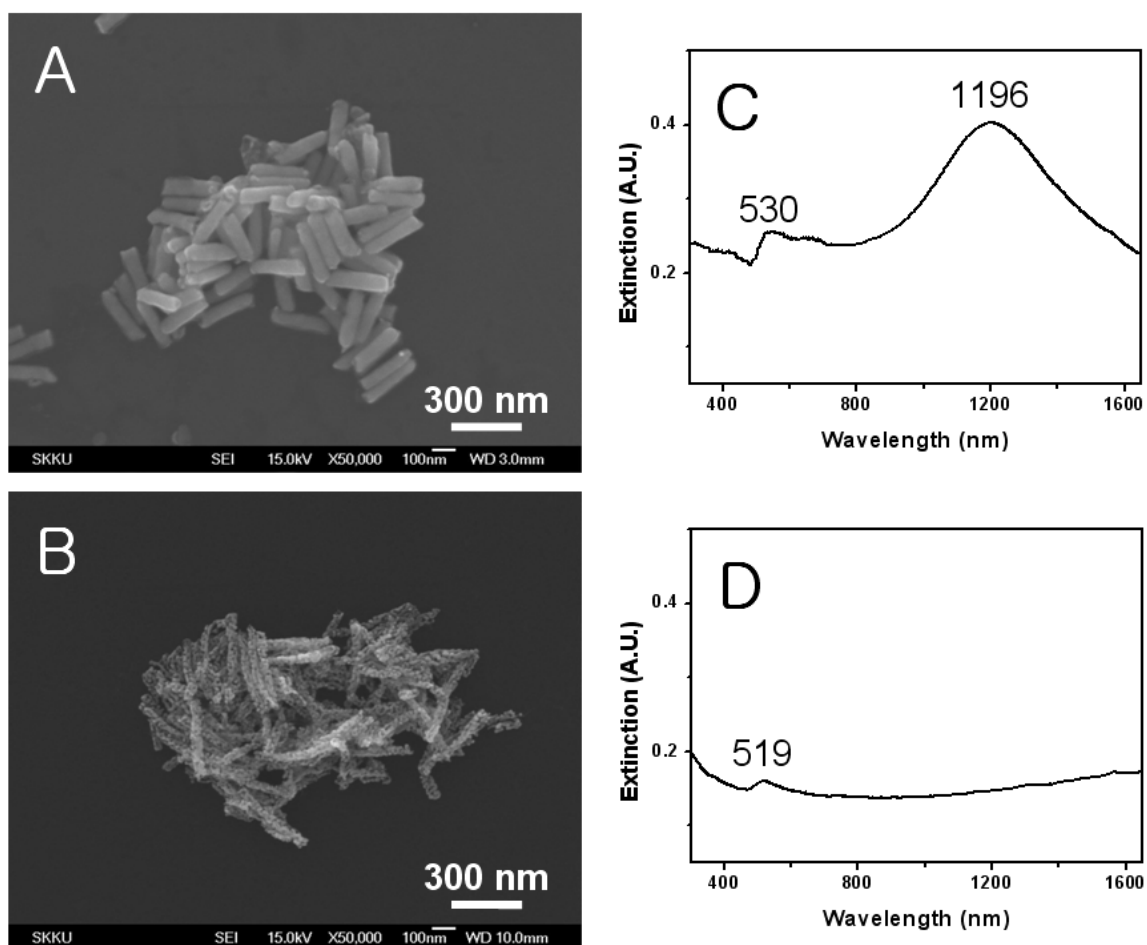
Smooth and Nanoporous Au NR Synthesis: A thin layer of Ag (~300 nm) was thermally evaporated onto one side of a nanoporous AAO template, which served as the working electrode in a three-electrode electrochemical cell after making physical contact with a glassy carbon electrode. A Pt wire and Ag/AgCl electrode were used as the counter and reference electrode, respectively. For smooth Au NRs, Au (from Technic Inc.) was then deposited into the empty space of AAO channels at -0.95 V. Depending on the total amount of charge, the length could be controlled. Typically, 0.03 C results in 100 nm of smooth NRs when the

exposed apparent surface area is 0.9 cm^2 . For nanoporous Au NRs, gold/silver alloy NRs were electrodeposited from a solution containing gold/silver ions (for $\text{Ag}_x/\text{Au}_{1-x}$ alloy NR ($0.5 < x < 0.8$), molar ratio). Molar ratio of plating solutions were adjusted by using $0.05 \text{ M KAu}(\text{CN})_2$ and $0.25 \text{ M Na}_2\text{CO}_3$ solution, and $0.05 \text{ M KAg}(\text{CN})_2$ and $0.25 \text{ M Na}_2\text{CO}_3$ solution. The electrochemical deposition potential was performed at a constant potential of -0.95 V . Ag component was selectively etched with concentrated nitric acid. As with the case of smooth NRs, the length could be controlled as a function of total amount of charge. Typically, when x is 0.6, 0.03 C results in 80 nm of nanoporous NRs, when the exposed apparent



surface area is 0.9 cm^2 . The NRs were then released from the template in an aqueous 3 M NaOH solution. The resulting NRs were rinsed with distilled water until the $\text{pH} \sim 7$. The rods were re-dispersed in D_2O for extinction spectrum characterization.

Fig. S1 Schematic representation of the synthesis of $\text{Au}_{\text{smooth}}/\text{Au}_{\text{nanoporous}}$ NRs. The electrochemical codeposition of Au^+ and Ag^+ results in Au/Ag alloy NRs in the interior of



AAO templates. The Ag and AAO components were dissolved with concentrated nitric acid and 3M NaOH solution, respectively.

Fig. S2 FESEM images of (A) pure smooth Au NRs (diameter = $70 (\pm 5)$ nm, length = $233 (\pm 20)$ nm) and (B) pure nanoporous Au NRs (diameter = $40 (\pm 4)$ nm, length = $290 (\pm 30)$ nm). (C) the corresponding UV-vis-NIR spectrum for (A). (D) for (B). Smooth Au NRs show the transverse and longitudinal dipole modes at 530 and 1196 nm, respectively. Nanoporous Au NRs show the transverse mode peak at 519 nm without any feature for longitudinal modes in the given spectral window. Spectra are un-normalized.

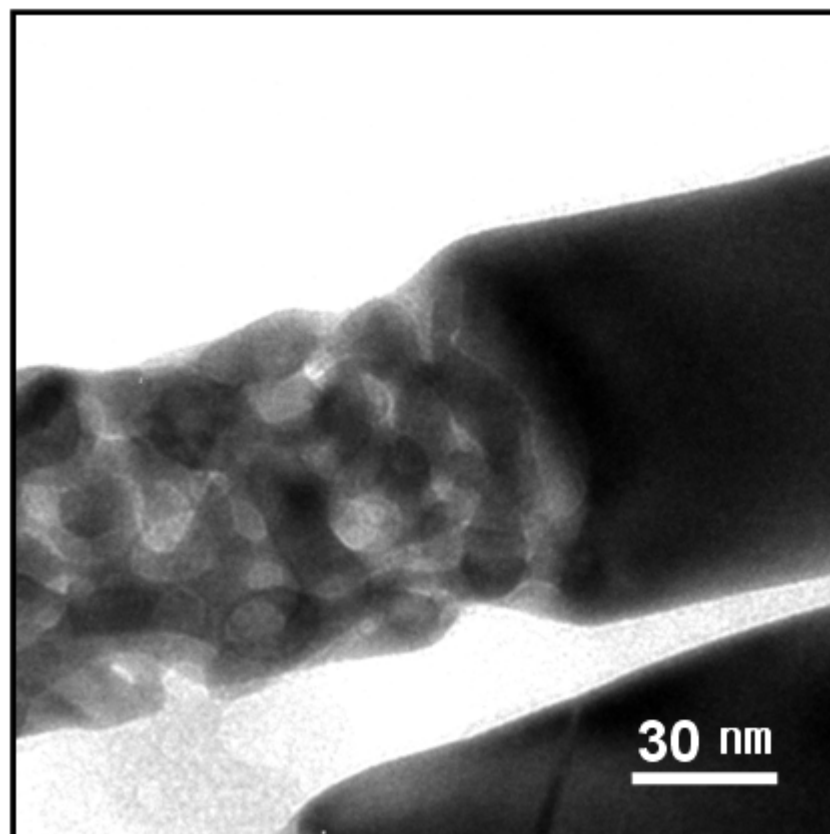


Fig. S3 A zoomed-in high resolution TEM image of $\text{Ag}_{0.6}/\text{Au}_{0.4}$ NR, showing the boundary between smooth and nanoporous domains after selective Ag etching.

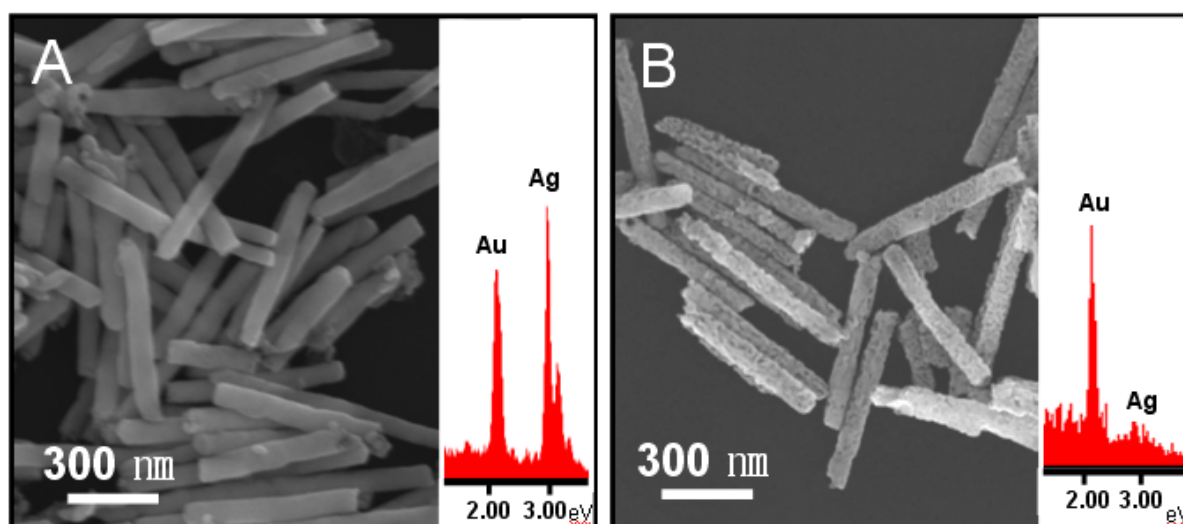


Fig. S4 FESEM images of smooth $\text{Ag}_{0.6}/\text{Au}_{0.4}$ NRs (A) before and (B) after Ag etching. Insets are the corresponding EDS spectrum. After Ag etching, most of Ag were dissolved but trace amount of Ag are evident in the ESD spectrum of nanoporous Au NRs.

DDA Calculations: We have calculated the optical properties of the Au NRs with both smooth and nanoporous surfaces using the Discrete Dipole Approximation (DDA) [s1,s2]. The particle is represented by an array of point dipoles. Each dipole obtains an oscillating polarization from the local field at that site given by

$$\mathbf{P}_j = \alpha_j \left[\mathbf{E}_j^{\text{inc}} - \sum_{k \neq j}^N \mathbf{A}_{jk} \mathbf{P}_k \right] \quad (1)$$

where α is the polarizability, \mathbf{E}^{inc} is the incident field, and \mathbf{A} is a dipole interaction matrix. The dipole polarizability incorporates the optical constants of Au [s3] and is assigned based on a lattice dispersion relation [s4]. The total field contains contributions from an incident plane wave

$$\mathbf{E}_j^{\text{inc}} = E_0 \exp(i\mathbf{k} \cdot \mathbf{r}_j - i\omega t) \quad (2)$$

and the field radiated from other dipoles in the array given by

$$\mathbf{A}_{jk} \mathbf{P}_k = \frac{\exp(ikr_{jk})}{r_{jk}^3} \left\{ k^2 \mathbf{r}_{jk} \times (\mathbf{r}_{jk} \times \mathbf{P}_k) + \frac{(1 - ikr_{jk})}{r_{jk}^2} \left[r_{jk}^2 \mathbf{P}_k - 3\mathbf{r}_{jk} (\mathbf{r}_{jk} \cdot \mathbf{P}_k) \right] \right\}. \quad (3)$$

The diagonal elements of matrix \mathbf{A} are assigned as α_j^{-1} , so the equation describing each lattice site can now be written as

$$\sum_{k=1}^N \mathbf{A}_{jk} \mathbf{P}_k = \mathbf{E}_j^{\text{inc}}, \quad (4)$$

where N is the number of dipoles in the array. The system of complex, linear equations can be succinctly represented by defining $3N$ -dimensional vectors \mathbf{P} and \mathbf{E}^{inc} , and a $3N \times 3N$ matrix \mathbf{A} giving the single matrix equation

$$\mathbf{A}\mathbf{P} = \mathbf{E}^{\text{inc}}. \quad (5)$$

For small numbers of dipoles matrix \mathbf{A} can be inverted to obtain the induced polarization matrix \mathbf{P} ; however, the matrix inversion is not feasible for the large number of dipoles needed to accurately represent most nanostructures. Alternatively, an iterative procedure is used to solve for the polarization of each dipole. The extinction cross section is then calculated via the optical theorem as

$$C_{\text{ext}} = \frac{4\pi k}{|\mathbf{E}^{\text{inc}}|^2} \sum_{j=1}^N \text{Im}\{\mathbf{E}_j^{\text{inc}*} \cdot \mathbf{P}_j\} \quad (6)$$

For the calculations, nanoporous structures were generated by randomly removing dipoles from smooth rod geometries. Lattice sites within three layers of the particle surface (i.e. volume elements within three dipole spacings) were allowed to be removed, as this distance is approximately the same scale as the prominent surface features present on the nanoporous NRs investigated experimentally. Previous calculations determined that the largest red shifts were produced when half of the eligible dipoles were removed [s5]. All of the simulation results presented on nanoporous NRs used this prescription for generating the structures.

REFERENCES

- S1. B. T. Draine, *Astrophys. J.* **333**, 848 (1988).
- S2. B. T. Draine, P. J. Flatau, *J. Opt. Soc. Am. A* **11**, 1491 (1994).
- S3. P. B. Johnson, R. W. Christy, *Phys. Rev. B* **6**, 4370 (1972).
- S4. B. T. Draine, J. Goodman, *Astrophys. J.* **405**, 685 (1993).
- S5. H.-M. Bok et al., *Nano Lett.* **8**, 2265 (2008).